J Appl Electrochem (2013) 43:1005–1010
DOI 10.1007/s10800-013-0589-3

RESEARCH ARTICLE

Gold nanoparticles deposited on amine functionalized silica sphere and its modified electrode for hydrogen peroxide sensing

Perumal Rameshkumar · Ramasamy Ramaraj

Received: 19 April 2013 / Accepted: 13 July 2013 / Published online: 28 July 2013

Abstract A facile and environmentally benign synthetic route to decorate preformed amine functionalized silica spheres (SiO_2) by in situ formation of gold nanoparticles (Au NPs) at three different concentrations (1, 2, and 3 mM) of Au precursor ($HAuCl_4$) is reported. UV–Visible absorption spectra of SiO_2@Au (1, 2, and 3 mM) NPs showed a characteristic surface plasmon resonance band due to the presence of Au NPs and transmission electron microscopic images confirmed that the Au NPs were accommodated on the surface of the amine functionalized SiO_2 spheres without aggregation. Herein, *N*-[3-(trimethoxysilyl) propyl] diethylenetriamine acted as both reducing and stabilizing agent for the Au NPs and no other protecting agents were used. Cyclic voltammogram recorded for the SiO_2@Au NPs modified glassy carbon (GC) electrode showed a characteristic electrochemical response due to the presence of Au NPs on the electrode. Electrocatalytic reduction of hydrogen peroxide (H_2O_2) was carried out at the SiO_2@Au (1, 2, and 3 mM) NPs modified GC electrodes, among which the SiO_2@Au (3 mM) NPs modified GC electrode produced the highest catalytic current. Electrochemical sensing of H_2O_2 was performed using linear sweep voltammetry at the SiO_2@Au (3 mM) NPs modified GC electrode with an experimental detection limit of 5 μM.

Keywords Silica spheres · Silicate sol–gel · Gold nanoparticles · Electrocatalysis · Hydrogen peroxide · Sensor

1 Introduction

Metal nanoparticles (NPs) have been widely investigated because of their unique optical and catalytic properties. Especially, gold (Au) and silver (Ag) NPs have attracted much attention due to their unique absorption features in the visible region of electromagnetic spectrum and their catalytic applications [1]. Moreover, the Au NPs and their ensembles of nanoelectrodes have found applications in electrocatalysis and sensors [2–5]. The development of different synthetic routes to prepare metal NPs dispersed in silicate sol–gel (SSG) is an important strategy because of their various applications in catalysis and sensors [6–10]. Lev and co-workers [7] demonstrated the encapsulation of metal nanoparticles by SSG. Silica (SiO_2) spheres are extensively used as a support material for metal NPs because they are inert in character and provide higher active surface area for accommodating metal NPs on their surface [11–16]. The metal NPs especially, Au and Ag NPs supported SiO_2 spheres are interesting materials due to their potential applications [15–19].

Hydrogen peroxide (H_2O_2) has got profound applications in pharmaceutical, clinical, environmental, mining, textile, and food manufacturing industries [20, 21]. It is a byproduct in many oxidative metabolic processes and also highly reactive oxygen species [20, 22, 23]. Hence, it is essential to develop sensors to detect H_2O_2 and electrochemical methods are extensively used for its sensing [24–27]. Furthermore, metal nanoparticles modified electrodes have recently been used as sensors for H_2O_2 [28–31].

Electronic supplementary material The online version of this article (doi:10.1007/s10800-013-0589-3) contains supplementary material, which is available to authorized users.

P. Rameshkumar · R. Ramaraj (✉)
Centre for Photoelectrochemistry, School of Chemistry, Madurai Kamaraj University, Madurai 625021, India
e-mail: ramarajr@yahoo.com

Previously, our group has reported the amperometric sensing of H_2O_2 using Au NPs [32] and core/shell Au/Ag NPs [33] embedded in SSG matrix. Au-coated SiO_2–fiber hybrid materials were also used for sensing of H_2O_2 [34].

In this report, we describe a facile and environmentally benign synthetic method to decorate preformed amine functionalized SiO_2 spheres by in situ formation of Au NPs at three different concentrations (1, 2, and 3 mM) of $HAuCl_4$ without using any external reducing or protecting agents. The electrocatalytic reduction of H_2O_2 was performed at the SiO_2@Au (1, 2, and 3 mM) NPs modified glassy carbon (GC) electrodes, among which the SiO_2@Au (3 mM) NPs modified GC electrode showed the best catalytic activity with an experimental detection limit of 5 μM.

2 Experimental

2.1 Materials and methods

Tetraethylorthosilicate (TEOS), *N*-[3-(trimethoxysilyl) propyl] diethylenetriamine (TPDT), and gold(III) chloride hydrate ($HAuCl_4$) were received from Sigma-Aldrich. H_2O_2 was purchased from Merck. All glassware was thoroughly cleaned with aqua regia (*Precaution: Aqua regia is a powerful oxidizing agent and it should be handled with extreme care*) and rinsed extensively with distilled water before use. Absorption spectra were recorded with an Agilent Technologies 8453 spectrophotometer using 1-cm quartz cell. Surface morphology of the nanomaterials was analyzed using the scanning electron microscopy (SEM) on a HITACHI (Model S-3400) instrument. High resolution transmission electron microscopy (HRTEM) images were recorded with a FEI TECNAI 30 G^2 S-TWIN instrument. Samples for TEM studies were prepared by placing a drop of fresh Au NPs on carbon coated copper grid and then evaporating the solvent under vacuum. Electrochemical measurements were performed at room temperature using a CH Instruments Electrochemical Workstation (Model-760D).

2.2 Synthesis of SiO_2@Au NPs

Amine functionalized TPDT SSG covered SiO_2 spheres were prepared by modified Stober method [14]. Briefly, ammonium hydroxide (1.7 mL; 25–28%) was added to ethanol (50 mL) along with TEOS (1.5 mL) and water (1 mL). The solution was stirred vigorously and after 3 h an additional 1 mL of TEOS was added. The SiO_2 spheres were obtained after 12 h of stirring and then TPDT (0.4 mL) was added to the solution and the stirring was continued for 6 h. The TPDT-functionalized SiO_2 particles were purified twice by centrifugation and redispersion in water (40 mL). In situ deposition of Au NPs on SiO_2 spheres was carried out by the following procedure. About 5 mg of preformed amine functionalized SiO_2 was added to 25 μL of 1 M TPDT silane in 5 mL of water and sonicated for 5 min. To this solution, $HAuCl_4$ (1 or 2 or 3 mM final concentrations) was added and stirred for 12 h. The appearance of wine red color indicated the formation of Au NPs on SiO_2 spheres.

2.3 Electrochemical measurements

Electrochemical measurements were conducted in a single compartment three-electrode cell. The working electrode was prepared by drop-casting 5 μL of TPDT SSG–SiO_2@Au NPs solution on GC electrode surface (3 mm dia.) and the thickness of the film was calculated as 1 μm. The GC electrode was cleaned by polishing twice with alumina (0.05 μm) and sonicated for 2 min before use. The calomel electrode and a platinum wire were used as reference and counter electrodes, respectively. The electrochemical measurements were performed at room temperature using a CH Instruments Electrochemical Workstation (Model-760D) in 0.1 M phosphate buffer solution (pH 7.2).

3 Results and discussion

3.1 Spectral characterization of SiO_2@Au NPs

The deposition of Au NPs on the TPDT functionalized SiO_2 spheres by in situ wet chemical synthesis was carried out using different concentrations of $HAuCl_4$ (1, 2, and 3 mM). Figure 1 displays the absorption spectra of colloidal solutions of SiO_2 (a), SiO_2@Au (1 mM) NPs (b), SiO_2@Au (2 mM) NPs (c), and SiO_2@Au (3 mM) NPs (d). The observed surface plasmon resonance (SPR) bands at 520, 542, and 531 nm corresponding to SiO_2@Au (1 mM), SiO_2@Au (2 mM), and SiO_2@Au (3 mM) NPs, respectively, indicate the presence of Au NPs on SiO_2 spheres and inset of Fig. 1 shows the wine red color for the SiO_2@Au (3 mM) NPs. It is known that the SPR absorption band of Au NPs is very sensitive to their size and local environment [35, 36]. The TPDT SSG acts as both reducing and stabilizing agent for the growth of Au NPs. The stability of the colloidal SiO_2@Au NPs was monitored by recording the absorption spectra over a period of 3 months and it was found that the Au NPs were very stable for more than 3 months. This suggests that the amine functionalized SiO_2 spheres provide comfortable accommodation for the Au NPs and the observed stability of the NPs can be ascribed to their interaction with the $–NH_2$ groups of TPDT.

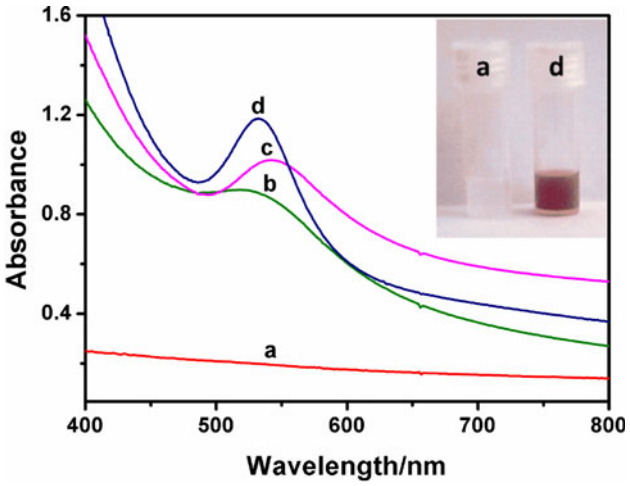

Fig. 1 UV–Visible absorption spectra obtained for colloidal solutions of SiO_2 spheres (**a**), SiO_2@Au (1 mM) NPs (**b**), SiO_2@Au (2 mM) NPs (**c**) and SiO_2@Au (3 mM) NPs (**d**). *Inset* photograph of SiO_2 (**a**) and SiO_2@Au (3 mM) NPs (**d**) solutions

3.2 HRTEM characterization of SiO_2@Au NPs

Figure 2 shows the HRTEM images of SiO_2@Au (1 mM) (a) and SiO_2@Au (3 mM) NPs (b) and they clearly demonstrate the deposition of Au NPs on SiO_2 spheres. The average size of SiO_2 spheres was calculated as ~250 nm (Fig. S1). It was observed from the HRTEM images that the shape of the deposited Au NPs was spherical in the case of SiO_2@Au (1 mM) NPs with an average size of 5.9 nm. In the case of SiO_2@Au (3 mM) NPs, the Au NPs were not perfectly spherical and most of the particles were hexagonal in shape with an average size of 36.2 nm. The size of the Au NPs in SiO_2@Au (3 mM) NPs was bigger than that in SiO_2@Au (1 mM) NPs due to the higher concentration of $HAuCl_4$. Aggregation and sedimentation of Au NPs were observed when the concentration of $HAuCl_4$ was increased above 4 mM. The HRTEM images of SiO_2@Au (1 and 3 mM) NPs at higher magnifications are shown in Fig. S2. The EDX analysis was carried out for the SiO_2@Au (3 mM) NPs and the peaks observed in the EDX spectrum confirmed the presence of Au content (Fig. S3). The crystal planes obtained from the SAED patterns match well with the values of Au in the JCPDS card number 65-2870. The (1 1 1), (2 0 0), (2 2 0) and (3 1 1) planes for SiO_2@Au (1 mM) NPs and (1 1 1), (2 0 0) and (3 1 1) planes for SiO_2@Au (3 mM) NPs were observed for Au (Fig. S4). Though SiO_2 spheres are amorphous in nature, the presence of Au NPs on the spheres gives the ring patterns in SAED. To our knowledge, a new synthetic procedure for the in situ deposition of Au NPs on amine functionalized SiO_2 spheres is reported for the first time.

3.3 Electrocatalysis of hydrogen peroxide

The electrochemical characteristic of the GC/TPDT–SiO_2@Au NPs modified electrode was studied using cyclic voltammetry. Figure 3 shows the comparison of cyclic voltammograms recorded for the GC/TPDT–SiO_2@Au (1 mM) NPs (a), GC/TPDT–SiO_2@Au (2 mM) NPs (b) and GC/TPDT–SiO_2@Au (3 mM) NPs (c) electrodes in 0.5 M H_2SO_4. The GC/TPDT–SiO_2@Au (3 mM) NPs (c) electrode showed a clear anodic peak and a cathodic peak at around 0.954 and 0.390 V, respectively corresponding to the oxidation of Au NPs into gold oxide and its reduction when compared to the GC/TPDT–SiO_2@Au (1 mM) NPs (a) and GC/TPDT–SiO_2@Au (2 mM) NPs (b) electrodes. This confirms the electrochemical characteristics of Au NPs at the modified GC electrode.

Figure 4 shows the cyclic voltammograms obtained for 1 mM H_2O_2 at the TPDT–SiO_2@Au (1 mM) NPs (a), TPDT–SiO_2@Au (2 mM) NPs (b), and TPDT–SiO_2@Au (3 mM) NPs (c) modified GC electrodes in 0.1 M

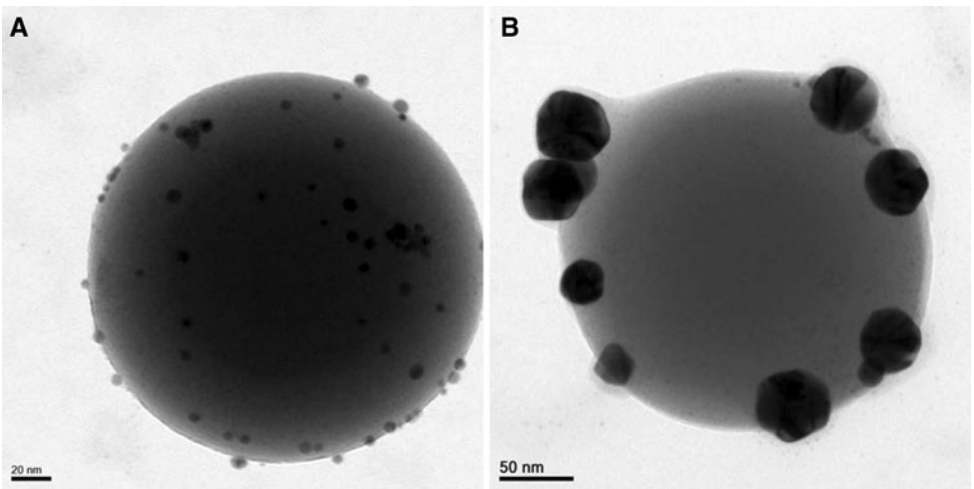

Fig. 2 HRTEM images of SiO_2@Au (1 mM) (**a**) and SiO_2@Au (3 mM) NPs (**b**)

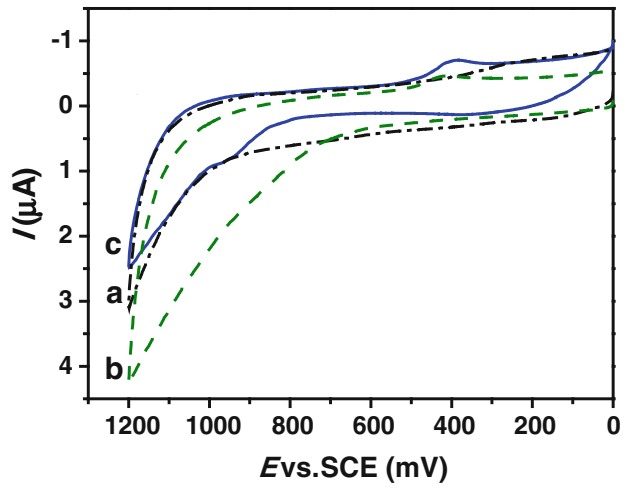

Fig. 3 Cyclic voltammograms recorded at GC/TPDT–SiO_2@Au (1 mM) NPs (**a**) (*dash dotted line*), GC/TPDT–SiO_2@Au (2 mM) NPs (**b**) (*dashed line*), and GC/TPDT–SiO_2@Au (3 mM) NPs (**c**) (*solid line*) electrodes in 0.5 M H_2SO_4 at a scan rate of 50 mV s^{-1}

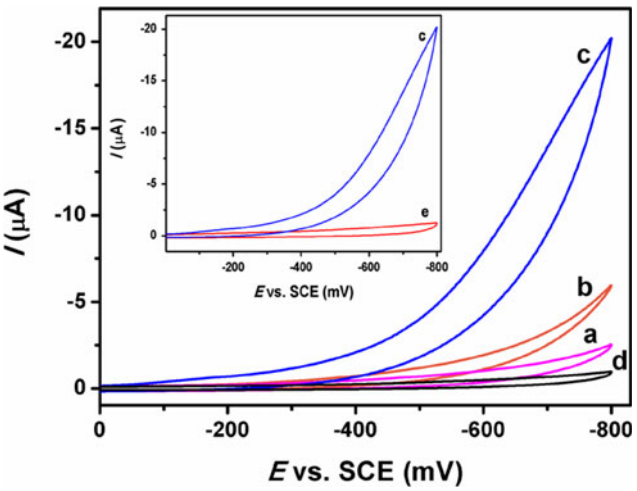

Fig. 4 Cyclic voltammograms recorded at GC/TPDT–SiO_2@Au (1 mM) NPs (**a**), GC/TPDT–SiO_2@Au (2 mM) NPs (**b**) GC/TPDT–SiO_2@Au (3 mM) NPs (**c**), and bare GC electrodes (**d**) for 1 mM H_2O_2 in 0.1 M phosphate buffer solution (pH 7.2) at a scan rate of 50 mV s^{-1}. *Inset* cyclic voltammograms recorded at GC/TPDT–SiO_2@Au (3 mM) NPs electrode in the absence (**e**) and presence (**c**) of 1 mM H_2O_2

phosphate buffer solution (pH 7.2). It is understood that the loading of Au NPs on amine functionalized SiO_2 spheres brings about the electrocatalytic reduction of H_2O_2 at the SiO_2@Au NPs modified electrodes. The GC/TPDT–SiO_2@Au (3 mM) NPs modified electrode exhibited excellent electrocatalytic activity toward the reduction of H_2O_2 and the catalytic reduction current started to appear at around −0.1 V (Fig. 4c). Inset of Fig. 4 shows the cyclic voltammograms obtained at GC/TPDT–SiO_2@Au (3 mM)

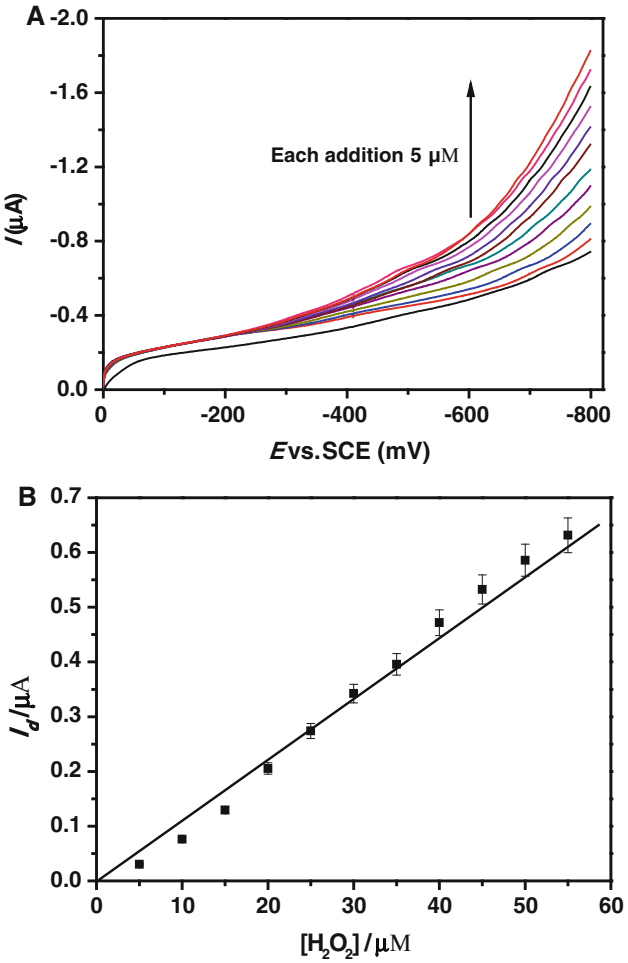

Fig. 5 Linear sweep voltammograms recorded at GC/TPDT–SiO_2@Au (3 mM) NPs electrode for each addition of 5 μM H_2O_2 (11 additions) in 0.1 M phosphate buffer solution (pH 7.2) at a scan rate of 50 mV s^{-1} (**a**) and their corresponding calibration plot with current measured at −0.7 V (**b**)

NPs electrode in the absence (e) and presence (c) of 1 mM H_2O_2. In the absence of H_2O_2, characteristic catalytic current was not observed. This observation clearly revealed that the Au NPs present on the SiO_2 spheres were responsible for the electrocatalytic reduction of H_2O_2 at the GC/TPDT–SiO_2@Au (3 mM) NPs modified electrode. The bare GC electrode did not show characteristic catalytic reduction current due to H_2O_2 reduction in the potential window (Fig. 4d). The cathodic peak currents observed at TPDT–SiO_2@Au (1 mM) NPs, TPDT–SiO_2@Au (2 mM) NPs and TPDT–SiO_2@Au (3 mM) NPs modified GC electrodes for 1 mM H_2O_2 were 1.6, 3.2, and 14.0 μA, respectively at −0.7 V. The electrocatalytic reduction of H_2O_2 was also carried out at GC/TPDT and GC/TPDT–SiO_2 modified electrodes in 0.1 M phosphate buffer solution (pH 7.2) (Fig. S5), where no catalytic reduction current was observed when compared to TPDT–SiO_2@Au (3 mM)

NPs modified electrode. These observations disclose that the Au NPs act as nanoelectrode for the electrocatalytic reduction of H_2O_2 with efficient electron transfer reaction.

3.4 Linear sweep voltammetric sensing of H_2O_2

Figure 5 shows the linear sweep voltammograms (LSV) recorded for each addition of 5 μM H_2O_2 at the GC/TPDT–SiO_2@Au (3 mM) NPs modified electrode. The voltammograms showed a significant increase in the reduction current during the successive addition of H_2O_2 (Fig. 5a) with linear relation (Fig. 5b). The sensitivity of the electrode toward the reduction of H_2O_2 was found as 0.0118 ± 0.00036 μA/μM.

Previous reports showed the lowest experimental detection limits of 2.5 μM, 10 μM, and 50 nM corresponding to Au NPs [32], core/shell Au/Ag NPs [33] and core/shell Au/Ag nanorods [37], respectively, embedded in SSG matrix modified electrodes for H_2O_2 using amperometric method. Shen et al. [34] reported a H_2O_2 sensor with an experimental detection limit of 2 μM using Au-coated SiO_2–fiber hybrid material. In this work, highly stable Au NPs deposited on amino-silicate functionalized SiO_2 spheres were prepared by a simple and environmentally benign synthetic method. The SiO_2@Au NPs modified electrode was used for the detection of H_2O_2 with an experimental detection limit of 5 μM using linear sweep voltammetric technique.

4 Conclusions

In conclusion, a simple and environmentally benign synthetic method to decorate preformed amine functionalized SiO_2 spheres by in situ formation Au NPs in the presence of TPDT SSG matrix was reported. No external reducing agents were used for the formation of Au NPs. The SiO_2@Au NPs were successfully characterized by UV–Visible absorption spectra, HRTEM, and EDX analysis. The TPDT acted as both reducing and stabilizing agent for the Au NPs. The electrocatalytic reduction of H_2O_2 was carried out at SiO_2@Au (1, 2, and 3 mM) NPs modified GC electrodes and the SiO_2@Au (3 mM) NPs modified GC electrode showed the highest catalytic current. The LSV studies demonstrated an experimental detection limit of 5 μM with catalytic reduction current of 0.0128 ± 0.00024 μA/μM for electrochemical sensing of H_2O_2. The SiO_2@Au NPs are a promising catalyst for a variety of electrocatalytic studies.

Acknowledgments The financial support from the Department of Science and Technology (DST), New Delhi, is gratefully acknowledged. The HRTEM images were recorded at PSG Institute of Advanced Studies, Coimbatore, India.

References

1. Tokonami S, Morita N, Takasaki K, Toshima N (2010) Novel synthesis, structure, and oxidation catalysis of Ag/Au bimetallic nanoparticles. J Phys Chem C 114:10336–10341. doi:10.1021/jp9119149
2. Daniel MC, Astruc D (2004) Gold nanoparticles: assembly, supramolecular chemistry, quantum-size-related properties, and applications toward biology, catalysis, and nanotechnology. Chem Rev 104:293–346. doi:10.1021/cr030698+
3. Dai X, Wildgoose GG, Salter C, Crossley A, Compton RG (2006) Electroanalysis using macro-, micro-, and nanochemical architectures on electrode surfaces. Bulk surface modification of glassy carbon microspheres with gold nanoparticles and their electrical wiring using carbon nanotubes. Anal Chem 78:6102–6108. doi:10.1021/ac060582o
4. Cheng W, Dong S, Wang E (2002) Colloid chemical approach to nanoelectrode ensembles with highly controllable active area fraction. Anal Chem 74:3599–3604. doi:10.1021/ac025661o
5. Szamocki R, Reculusa S, Ravaine S, Bartlett PN, Kuhn A, Hempelmann R (2006) Tailored mesostructuring and biofunctionalization of gold for increased electroactivity. Angew Chem Int Ed 45:1317–1321. doi:10.1002/anie.200503292
6. Maduraiveeran G, Ramaraj R (2009) Potential sensing platform of silver nanoparticles embedded in functionalized silicate shell for nitroaromatic compounds. Anal Chem 81:7552–7560. doi:10.1021/ac900781d
7. Bharathi S, Fishelson N, Lev O (1999) Direct synthesis and characterization of gold and other noble metal nanodispersions in sol−gel-derived organically modified silicates. Langmuir 15:1929–1937. doi:10.1021/la980490x
8. Manivannan S, Ramaraj R (2011) Polymer-embedded gold and gold/silver nanoparticle modified electrodes and their applications in catalysis and sensors. Pure Appl Chem 83:2041–2053. doi:10.1351/PAC-CON-11-03-04
9. Lev O, Wu Z, Bharathi S, Glezer V, Modestov A, Gun J, Rabinovich L, Sampath S (1997) Sol−gel materials in electrochemistry. Chem Mater 9:2354–2375. doi:10.1021/cm970367b
10. Pandikumar A, Murugesan S, Ramaraj R (2010) Functionalized silicate sol−gel-supported TiO_2−Au core−shell nanomaterials and their photoelectrocatalytic activity. ACS Appl Mater Interfaces 2:1912–1917. doi:10.1021/am100242p
11. Rodolfo Z, Alberto S, Patricia S, Vladimir AB, Jose MS (2006) New preparation method of gold nanoparticles on SiO_2. J Phys Chem B 110:8559–8565. doi:10.1021/jp060601y
12. Pol VG, Srivastava DN, Palchik O, Palchik V, Slifkin MA, Weiss AM, Gedanken A (2002) Sonochemical deposition of silver nanoparticles on silica spheres. Langmuir 18:3352–3357. doi:10.1021/la0155552
13. Pol VG, Gedanken A, Calderon-Moreno J (2003) Deposition of gold nanoparticles on silica spheres: a sonochemical approach. Chem Mater 15:1111–1118. doi:10.1021/cm021013+
14. Guo S, Zhai J, Fang Y, Dong S, Wang E (2008) Nanoelectrocatalyst based on high-density Au/Pt hybrid nanoparticles supported on a silica nanosphere. Chem Asian J 3:1156–1162. doi:10.1002/asia.200700422
15. Yen C-W, Lin M-L, Wang A, Chen S-A, Chen J-M, Mou C-Y (2009) CO oxidation catalyzed by Au−Ag bimetallic nanoparticles supported in mesoporous silica. J Phys Chem C 113:17831–17839. doi:10.1021/jp9037683
16. Jean R-D, Chiu K-C, Chen T-H, Chen C-H, Liu D-M (2010) Functionalized silica nanoparticles by nanometallic Ag decoration for optical sensing of organic molecule. J Phys Chem C 114:15633–15639. doi:10.1021/jp106185m

17. Jiang Z-J, Liu C-Y, Sun L-W (2005) Catalytic properties of silver nanoparticles supported on silica spheres. J Phys Chem B 109:1730–1735. doi:10.1021/jp046032g
18. Kim YH, Lee DK, Cha HG, Kim CW, Kang YS (2007) Synthesis and characterization of antibacterial Ag−SiO_2 nanocomposite. J Phys Chem C 111:3629–3635. doi:10.1021/jp068302w
19. Kim YH, Kim CW, Cha HG, Lee DK, Jo BK, Ahn GW, Hong ES, Kim JC, Kang YS (2009) Bulklike thermal behavior of antibacterial Ag−SiO_2 nanocomposites. J Phys Chem C 113:5105–5110. doi:10.1021/jp809892c
20. Tsiafoulis CG, Trikalitis PN, Prodromidis MI (2005) Synthesis, characterization and performance of vanadium hexacyanoferrate as electrocatalyst of H_2O_2. Electrochem Commun 7:1398–1404. doi:10.1016/j.elecom.2005.10.001
21. Chen W, Cai S, Ren Q-Q, Wen W, Zhao Y-D (2012) Recent advances in electrochemical sensing for hydrogen peroxide: a review. Analyst 137:49–58. doi:10.1039/C1AN15738H
22. Wen Z, Ci S, Li J (2009) Pt nanoparticles inserting in carbon nanotube arrays: nanocomposites for glucose biosensors. J Phys Chem C 113:13482–13487. doi:10.1021/jp902830z
23. Ahmad M, Pan C, Gan L, Nawaz Z, Zhu J (2010) Highly sensitive amperometric cholesterol biosensor based on Pt-incorporated fullerene-like ZnO nanospheres. J Phys Chem C 114: 243–250. doi:10.1021/jp9089497
24. Wang J (2006) Electrochemical biosensors: towards point-of-care cancer diagnostics. Biosens Bioelectron 21:1887–1892. doi:10.1016/j.bios.2005.10.027
25. Jia WZ, Guo M, Zheng Z, Yu T, Rodriguez EG, Wang Y, Lei Y (2009) Electrocatalytic oxidation and reduction of H_2O_2 on vertically aligned Co_3O_4 nanowalls electrode: toward H_2O_2 detection. J Electroanal Chem 625:27–32. doi:10.1016/j.jelechem.2008.09.020
26. Pena RC, Gamboa JCM, Bertotti M, Paixao TRLC (2011) Studies on the electrocatalytic reduction of hydrogen peroxide on a glassy carbon electrode modified with a ruthenium oxide hexacyanoferrate film. Int J Electrochem Sci 6:394–403
27. Luo Y, Liu H, Rui Q, Tian Y (2009) Detection of extracellular H_2O_2 released from human liver cancer cells based on TiO_2 nanoneedles with enhanced electron transfer of cytochrome *c*. Anal Chem 81:3035–3041. doi:10.1021/ac802721x
28. Yin J, Qi X, Yang L, Hao G, Li J, Zhong J (2011) A hydrogen peroxide electrochemical sensor based on silver nanoparticles decorated silicon nanowire arrays. Electrochim Acta 56:3884–3889. doi:10.1016/j.electacta.2011.02.033
29. Lee YJ, Park JY, Kim Y, Ko JW (2011) Amperometric sensing of hydrogen peroxide via highly roughened macroporous gold-/platinum nanoparticles electrode. Curr Appl Phys 11:211–216. doi:10.1016/j.cap.2010.07.009
30. Li Y, Lu Q, Wu S, Wang L, Shi X (2013) Hydrogen peroxide sensing using ultrathin platinum-coated gold nanoparticles with core@shell structure. Biosens Bioelectron 41:576–581. doi:10.1016/j.bios.2012.09.027
31. Li X, Heryadi D, Gewirth AA (2005) Electroreduction activity of hydrogen peroxide on Pt and Au electrodes. Langmuir 21:9251–9259. doi:10.1021/la0508745
32. Maduraiveeran G, Ramaraj R (2007) Gold nanoparticles embedded in silica sol–gel matrix as an amperometric sensor for hydrogen peroxide. J Electroanal Chem 608:52–58. doi:10.1016/j.jelechem.2007.05.009
33. Manivannan S, Ramaraj R (2009) Core–shell Au/Ag nanoparticles embedded in silicate sol–gel network for sensor application towards hydrogen peroxide. J Chem Sci 121:735–743
34. Shen J, Yang X, Zhu Y, Kang H, Cao H, Li C (2012) Gold-coated silica–fiber hybrid materials for application in a novel hydrogen peroxide biosensor. Biosens Bioelectron 34:132–136. doi:10.1016/j.bios.2012.01.031
35. Prasad BL, Sorensen CM, Klabunde KJ (2008) Gold nanoparticle superlattices. Chem Soc Rev 37:1871–1883. doi:10.1039/B712175J
36. Kelly KL, Coronado E, Zhao LL, Schatz GC (2003) The optical properties of metal nanoparticles: the influence of size, shape, and dielectric environment. J Phys Chem B 107:668–677. doi:10.1021/jp026731y
37. Jayabal S, Ramaraj R (2013) Synthesis of core/shell Au/Ag nanorods embedded in functionalized silicate sol–gel matrix and their applications in electrochemical sensors. Electrochim Acta 88:51–58. doi:10.1016/j.electacta.2012.10.065